Transmembrane Distribution of Membrane Constituents in Organic Nanotubes Driven by Electric Charge and Intrinsic Anisotropy of Molecules

Klemen Bohinc,*,†,‡ Tomaž Slivnik,† Aleš Iglič,† Milan Brumen,§,|| and Veronika Kralj-Iglič⊥

Laboratory of Physics, Faculty of Electrical Engineering, University of Ljubljana, Tržaška 25, SI-1000 Ljubljana, Slovenia, Department of Physiotherapy, College of Health Studies, University of Ljubljana, Poljanska 26a, 1000 Ljubljana, Slovenia, Faculty of Natural Sciences and Mathematics, and Medical Faculty, University of Maribor, Slomškov trg 15, SI-2000 Maribor, Slovenia, Jožef Stefan Institute, Jamova 39, SI-1000 Ljubljana, Slovenia, and Laboratory of Clinical Biophysics, Faculty of Medicine, University of Ljubljana, Lipičeva 2, SI-1000 Ljubljana, Slovenia

Received: December 22, 2006; In Final Form: April 29, 2007

The transmembrane distribution of membrane constituents in the two leaflets of a cylindrical bilayer, which is in contact on both sides with an electrolyte solution, was studied by mathematical modeling. The model considers electrostatic interactions between the charged membrane molecules and the monovalent ions of the electrolyte solution, the bending elasticity of the membrane, as well as the anisotropy of the molecular intrinsic shape in the membrane. We showed that the strongly anisotropic uncharged membrane constituents are distributed asymmetrically between the two leaflets of the membrane. The asymmetric transmembrane distribution of charged weakly anisotropic membrane constituents is caused by the difference between the ionic strengths in the outer solutions and those in the inner solutions. For strongly anisotropic charged constituents in the membrane, we found that the asymmetric transmembrane distribution is driven by an interplay between the shape and the charge of the membrane constituents, as well as the difference between the ionic strengths in the outer solutions and those in the inner solutions. We also showed that the composition of the bilayer and the intrinsic curvatures of membrane components influence the stability of the tube.

1. Introduction

Thin tubular organic structures have become a subject of increasing interest due to their importance in biology and technology.[1−3] They are often formed by biological membranes.[4−6] Polymerization of actin and microtubules into long filaments beneath the cell membrane is assumed to be one of the possible origins of protrusive force which is supposed to push out the cell membrane in the form of thin tubular membrane protrusion.[7−10] It is also thought that the tubular structures can be formed by membrane associated motor proteins which are able to grab the membrane and pull on it as they move along the cytoskeletal filaments.[11] In experiments, the techniques as optical tweezers[12] or micropipettes[13] are also able to produce the tubular membrane structures.

It was shown that long and thin tubular membrane protrusions can be stable also without an inner supporting rod-like structure or a pulling mechanical force.[14,15] As an example, the tubular budding of biological membranes is possible also because of the accumulation of anisotropic membrane constituents in the tubular membrane region.[15,16] Without the accumulation of anisotropic membrane constituents and without the protrusive force, the spherical budding is always energetically favorable.[17,18,15]

The mechanism of tubular budding may also be responsible for stabilization of the thin tubes that connect cells or cell organelles[5,6] and might be important for transport of matter and information in cellular systems.[2−4,6,19] Some recent studies indicated that vesicular transport between cell organelles over longer distances is not random and that it takes place between specific surface regions of the cell organelles.[20,1] Among other mechanisms, such an organized transport may be achieved by nanotube-directed transport of carrier vesicles or direct transport through nanotubes.[2,19,4,6] Such nanotubes constituted of cell membrane link two cells and open communication between them. Both immune and neural cells have been observed to transfer proteins or calcium to one another through these nanotunnels, and viruses have been seen to travel from cell to cell within the tube as well.[21] Thin tubular membraneous structures are therefore important in cell structure and function,[2,4−6] but they have not been extensively explored in the past because of experimental difficulties in investigating these thin and fragile structures. Therefore, very little is known about the variables that control their shape or the distribution of lipid molecules between the two membrane layers.[22,14,15]

The components of biological membranes are asymmetrically distributed between the two surfaces. Almost every type of lipid is present on both sides of the membrane bilayer but in different amounts.[23] There are many reasons for the asymmetric distribution of components between the two layers and different possible explanations. For example, in the erythrocyte membrane, the asymmetric distribution of lipids can be partially ascribed to interactions of lipids with spectrin.[24] On the other hand, there is experimental and theoretical evidence that an asymmetric distribution of lipids between the membrane layers is an ATP-dependent process.[25,26] It was observed that ATP-dependent translocation of phosphatidylserine and phosphatidylethanola-

* Corresponding author. Phone: +386-1-4768-235. Fax: +386-1-4768-850. E-mail: klemen.bohinc@fe.uni-lj.si.
† Laboratory of Physics, University of Ljubljana.
‡ Department of Physiotherapy, University of Ljubljana.
§ University of Maribor.
|| Jozef Stefan Institute.
⊥ Laboratory of Clinical Biophysics, University of Ljubljana.

10.1021/jp068889e CCC: $37.00
Published on Web 06/20/2007

mine molecules from the outer membrane monolayer to the cytoplasmic one takes place. Furthermore, a theoretical study of phospholipid translocation in the erythrocyte membrane, taking into account active and passive fluxes of these lipids and passive fluxes of phosphatidylcholine, sphingomyeline, and cholesterol, showed that an asymmetric lipid distribution emerges from counterbalanced fluxes whereby the passive fluxes are driven by concentration gradients and by mechanical forces arising from an area limitation of lipid occupation in both membrane layers.[27]

The lateral and transmembrane distribution of lipid and protein molecules in bilayer membrane structures exhibiting high membrane curvatures may strongly depend on the intrinsic shape of the constituent molecules.[28,29] Israelachvili et al.[28] have shown that the up−down asymmetry of the lipid molecules, that is, the relative size of their head group and hydrophobic tails, are the major lipid properties that determine asymmetry in the transmembrane distribution of lipids in two-component very small spherical vesicles.[30]

Normally, the constituents of biological membranes (lipids, glycoproteins, glycolipids, etc.) carry one or more ionized or polar groups.[31] The ionized groups contribute to the surface charge density. The molecules which are bound to or absorbed onto the membrane surface may also contribute to the surface charge density.[32] Therefore, the electrostatic interactions between the membrane surface charge and the ions in solution may influence the distribution of charged components between the leaflets of the membrane and the concentration profile of the ions in the electrolyte solution inside and outside the membrane (tube).[33]

In this work, the transmembrane distribution of membrane constituents is studied theoretically for two-component membrane bilayer nanotubes having high membrane curvature. Therefore, in contrast to previous studies[28] where only isotropic intrinsic curvatures of the membrane components were considered, in the present work, we take into account the fact that the membrane components may in general also be anisotropic with respect to the axis pointing in the direction of the normal to the membrane bilayer.[34,35]

The membrane bilayer nanotubes composed of charged and uncharged constituents in general may have different surface charge densities on the inner and outer surfaces. This asymmetry causes different surface potentials in the inner and outer surfaces. In order to describe such systems, a theoretical model was constructed, which allows the area densities of membrane constituents to equilibrate between the inner and the outer membrane monolayers. Additionally, the exchange of counterions from the inside to the outside of the nanotube and vice versa was taken into account; this is needed to fulfill the electroneutrality condition of the whole system.

Starting from a microscopic description of the intrinsic shape of membrane constituents, we derived an expression for the membrane-free energy taking into account the orientational ordering of the anisotropic membrane constituents. In our model, the membrane free energy involves the electrostatic free energy of the charged membrane in contact with the inner and outer electrolyte solutions and the deviatoric contribution of the individual anisotropic membrane constituents because of their orientational ordering.[34,36,37] From the condition for the free energy to reach its minimum, the equilibrium transmembrane distributions of charged and neutral tube components were predicted for different values of model parameters such as the mean curvature and curvature deviator of the intrinsic molecular shape, the charge of the membrane constituents, the lateral interaction constant of a single molecule within the surrounding layer, and the ionic strengths in the inner and the outer electrolyte solution.

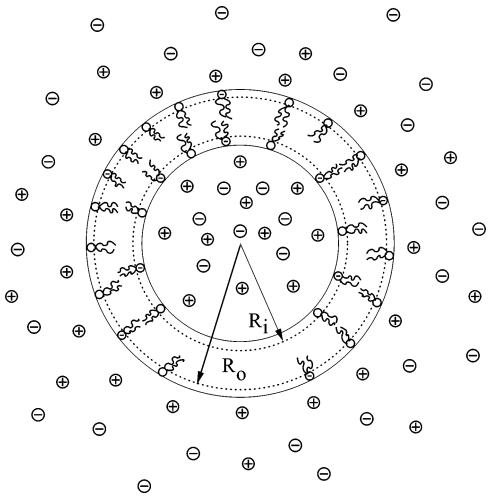

Figure 1. Schematic presentation of the cross section of a bilayer nanotube, which is in contact outside and inside with the electrolyte solution.

For the sake of simplicity, we restricted our theoretical considerations to the stable tubular structures which are possible only at high enough lateral membrane tensions. Namely, at high membrane lateral tension, the membrane fluctuations (and/or undulations) around the average tubular shape are largely suppressed.[38] Such high lateral tension may be achieved either by an inner supporting cytoskeleton rod-like structure or by a pulling mechanical force produced by the techniques such as optical tweezers.[12,8−10]

2. Theory

We consider a tube with the membrane built up from two monolayers. The symbols R_o and R_i denote the outer and the inner radii of the tube (Figure 1), respectively. The length (l) of the tube is assumed to be much larger than both radii. The membrane bilayer consists of two kinds of constituents. The molecules of the first type have intrinsic curvatures $C_{1m,1}$ and $C_{2m,1}$, while the molecules of the second type have intrinsic curvatures $C_{1m,2}$ and $C_{2m,2}$.[35] We shall assume that the molecules of the first type can in general have a net charge Z_1e_0, where $Z_1 = 0, \pm1, \pm2,..$, while the molecules of the second type always have zero net charge ($Z_2 = 0$).

The tube is coaxially enclosed in a cylindrical cell of radius R_{cell}. The tube is in contact inside and outside with a monovalent electrolyte solution. The ions with charge of the same sign as the tube are attracted by the membrane of the tube and are called counterions. The ions with a charge of the opposite sign to the tube are depleted from the tube and are called coions. A diffuse electrical double layer is created inside and outside the tube. At the distance R_{cell} from the center of the tube, the electric field vanishes. For reasons of symmetry, the electric field must vanish at the tube axis.

The total number of molecules in the outer layer N_o is

$$N_o = N_1 + N_2 \tag{1}$$

where N_1 is the number of molecules of the first type and N_2 is the number of molecules of the second type in the outer layer, while the total number of molecules in the inner layer N_i is

$$N_i = \tilde{N}_1 + \tilde{N}_2 \tag{2}$$

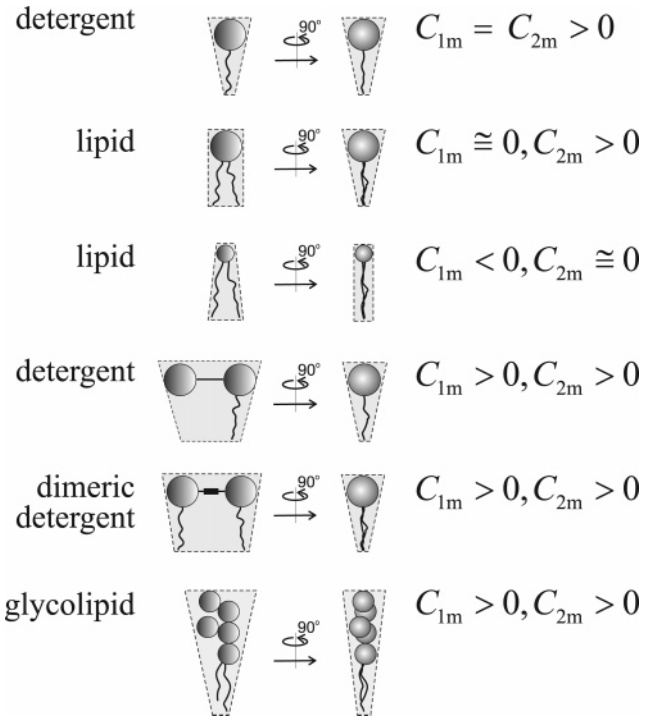

Figure 2. Schematic figure of intrinsic shapes of lipids, dimeric detergent, and glycolipid. Note that the values of intrinsic curvatures C_{1m} and C_{2m} do not necessary describe only the geometrical shape of the molecules (shaded region).

where $\tilde{N}_1$ is the number of molecules of the first type and $\tilde{N}_2$ is the number of molecules of the second type in the inner layer.

The number of molecules of the first type in the outer layer is given by $N_o = 2\pi R_o l/a$, where the outer radius of the tube is $R_o = R + \delta/2$, R is the mid-cylinder radius, δ is the thickness of the hydrophobic part of the lipid double layer, and a is the surface area of one lipid molecule. The number of molecules in the inner layer is given by $N_i = 2\pi R_i l/a$, where the inner radius of the cylinder is $R_i = R - \delta/2$.

The total number of molecules of the first type in the tube N_{1T} is

$$N_{1T} = N_1 + \tilde{N}_1 \tag{3}$$

Equations 1, 2, and 3 determine the total number of molecules of the second type in the tube $N_{2T} = N_2 + \tilde{N}_2 = N_o + N_i - N_{1T}$.

The anisotropic membrane constituent (Figure 2) can orient in the plane of the membrane according to the local membrane curvature.[34,36] The coupling between the orientation of the constituent and the difference between the two principal membrane curvatures causes orientational ordering in the regions where the difference between the two principal curvatures is large. The orientation of a constituent is given by rotation of the principal directions of the intrinsic constituent shape with respect to the membrane principal directions ω. The energy of a single molecule embedded in the bilayer nanotube is taken into account by[36]

$$W_i = \frac{\xi_i}{2}(H - H_{m,i})^2 + \frac{1}{2}\frac{\xi_i + \xi_i^*}{2}(D^2 - 2DD_{m,i}\cos 2\omega + {D_{m,i}}^2) \tag{4}$$

where $H = (C_1 + C_2)/2$ is the mean curvature of the tube, $D = |C_1 - C_2|/2$ is the curvature deviator of the tube, and C_1 and C_2 are the principal curvatures of the membrane. $H_{m,i} = (C_{1m,i} + C_{2m,i})/2$ and $D_{m,i} = (C_{1m,i} - C_{2m,i})/2$ are the mean curvature and the curvature deviator describing the intrinsic shape of a single molecule,[35,36] respectively. The strength of the interaction between a single molecule of type i and the surrounding membrane nanotube is represented by the constants ξ_i^* and ξ_i. The curvature energy is included through the energy of a single molecule (eq 4). In the limit of isotropic lipid molecules ($D_{m,i} = 0$), the described approach leads to the well-known Helfrich local bending energy of the lipid bilayer.[37]

In the case of spherical nanovesicles, it was shown that, ignoring any specific interactions between the lipids in the two-component vesicles, the equilibrium area of the lipids will remain close to their optimal areas.[28] For the sake of simplicity, in this work, the expression for the single-molecule energy (eq 4) does not involve the term[28,39,27] dependent on the area of the constituent molecule.

All molecules of a chosen type are considered to be indistinguishable. The partition function for the molecules in the outer membrane layer is given by

$$Q_o = \frac{N_o! {q_1}^{N_1} {q_2}^{N_2}}{N_1! N_2!} \tag{5}$$

while the partition function for molecules in the inner layer is given by

$$Q_i = \frac{\tilde{N}_i! {\tilde{q}_1}^{\tilde{N}_1} {\tilde{q}_2}^{\tilde{N}_2}}{\tilde{N}_1! \tilde{N}_2!} \tag{6}$$

where

$$q_i = e^{-(\xi_i/2kT)(H-H_{m,i})^2 - (\xi_i+\xi_i^*/4kT)(D^2+D_{m,i}^2) + \ln I_0((\xi_i+\xi_i^*)DD_{m,i}/2kT)} \tag{7}$$

is obtained through statistical averaging over all available orientations ω, kT is the thermal energy, and I_0 is the modified Bessel function. Inserting eq 5 into relation $F_o^m = -kT\ln Q_o$ and using the Stirling approximation, we obtain the free energy of the outer layer of the nanotube

$$F_o^m = kTN_1 \ln\frac{N_1}{N_o} + kTN_2 \ln\frac{N_2}{N_o} + N_1\alpha_1 + \alpha_2 N_2 \tag{8}$$

where

$$\alpha_j = \frac{\xi_j}{2}\left(\frac{1}{2R_o} - H_{m,j}\right)^2 + \frac{(\xi_j + \xi_j^*)}{4}\left(\left(\frac{1}{2R_0}\right)^2 + {D_{m,j}}^2\right) - kT \ln I_0\left(\frac{(\xi_j + \xi_j^*)D_{m,j}}{4R_o kT}\right) \tag{9}$$

We took into account that the curvature deviator of the outer layer of the tube $D = 1/(2R_o)$, while its mean curvature $H = 1/(2R_o)$.

Inserting eqs 6 into relation $F_i^m = -kT \ln Q_i$ and using the Stirling approximation, we obtain the free energy of the inner layer of the vesicle

$$F_i^m = kT\tilde{N}_1 \ln\frac{\tilde{N}_1}{N_i} + kT\tilde{N}_2 \ln\frac{\tilde{N}_2}{N_i} + \beta_1\tilde{N}_1 + \beta_2\tilde{N}_2 \tag{10}$$

where

$$\beta_j = \frac{\xi_j}{2}\left(-\frac{1}{2R_i} - H_{m,j}\right)^2 + \frac{(\xi_j + \xi_j^*)}{4}\left(\left(\frac{1}{2R_i}\right)^2 + {D_{m,j}}^2\right) - kT \ln I_0\left(\frac{(\xi_j + \xi_j^*)D_{m,j}}{4R_i kT}\right) \quad (11)$$

We have taken into account the fact that the curvature deviator of the inner layer of the tube $D = 1/2R_i$, while its mean curvature $H = 1/2R_i$.

The outer part of the tube is in contact with the electrolyte solution composed of monovalent counterions and coions with concentration n_d^o in the bulk, while the inner part of the vesicle is in contact with the electrolyte solution composed of counterions and coions with concentration n_d^i in the center. The electrostatic interaction between the ions in the electrolyte solution and the corresponding charged surface is taken into account within the linearized Poisson−Boltzmann (PB) theory. The electrostatic free energy of the outer electric double layer in the linearized PB theory[33,40] is given by

$$F_o^{el} = \frac{1}{2}\sigma_o \Phi(R_o) 2\pi R_o l \quad (12)$$

while the electrostatic free energy of the inner electric double layer[33] can be written as

$$F_i^{el} = \frac{1}{2}\sigma_i \Phi(R_i) 2\pi R_i l \quad (13)$$

where the electrostatic potential at the outer charged surface is given by (see Appendix)

$$\Phi(R_o) = c\sigma_o \frac{K_0(\kappa_o R_o)}{K_1(\kappa_o R_o)} \quad (14)$$

and

$$\sigma_o = -\frac{N_1 Z_1 e_0}{2\pi R_o l} \quad (15)$$

is the surface charge density of the outer layer, Z_1 is the valency of the membrane constituents of first type, e_0 is the elementary charge, $c = \sqrt{kT/(2e_0^2 n_d^o N_A \epsilon\epsilon_0)}$, N_A is Avogadro's number, ϵ is the relative dielectric constant of the solution, ϵ_0 is the permittivity of a vacuum, K_j are hyperbolic Bessel functions of order j, and $\kappa_o = \sqrt{2e_0^2 n_d^o N_A/(\epsilon\epsilon_0 kT)}$. The electrostatic potential at the inner charged surface in the linearized PB theory is given by (see Appendix)

$$\Phi(R_i) = \tilde{c}\sigma_i \frac{I_0(\kappa_i R_i)}{I_1(\kappa_i R_i)} \quad (16)$$

where

$$\sigma_i = -\frac{\tilde{N}_1 Z_1 e_o}{2\pi R_i l} \quad (17)$$

is the surface charge density of the inner layer, $\tilde{c} = \sqrt{kT/(2e_0^2 n_d^i N_A \epsilon\epsilon_0)}$, I_j are the modified Bessel functions of order j, and $\kappa_i = \sqrt{2e_0^2 n_d^i N_A/(\epsilon\epsilon_0 kT)}$.

The free energy of the whole system is thus given by:

$$F = F_o^m + F_o^{el} + F_i^m + F_i^{el} \quad (18)$$

According to Gauss's law, the energy of the bilayer is not considered (see eqs A.8 and A.17).

Inserting eqs 8, 10, 12, and 13 into eq 18, we obtain

$$F = kTN_1 \ln\frac{N_1}{N_o} + kT(N_o - N_1)\ln\frac{(N_o - N_1)}{N_o} + N_1\alpha_1 + (N_o - N_1)\alpha_2 + kT(N_{1T} - N_1)\ln\frac{(N_{1T} - N_1)}{N_i} + kT(N_i - N_{1T} + N_1)\ln\frac{(N_i - N_{1T} + N_1)}{N_i} + (N_{1T} - N_1)\beta_1 + (N_i - N_{1T} + N_1)\beta_2 + \frac{ce_0^2 N_1^2 Z_1^2}{4\pi R_o l}\frac{K_0(\kappa_o R_o)}{K_1(\kappa_o R_o)} + \frac{\tilde{c}e_0^2(N_{1T} - N_1)^2 Z_1^2}{4\pi R_i l}\frac{I_0(\kappa_i R_i)}{I_1(\kappa_i R_i)} \quad (19)$$

The number of molecules of first type N_1 in the outer layer can be determined by the condition for the free energy (eq 19) to be at its minimum

$$\frac{\partial F}{\partial N_1} = 0 \quad (20)$$

Inserting eq 19 into eq 20, we obtain the nonlinear equation for the equilibrium number N_1

$$kT\ln\frac{N_1(N_i - N_{1T} + N_1)}{(N_o - N_1)(N_{1T} - N_1)} + \alpha_1 - \alpha_2 - \beta_1 + \beta_2 + \frac{N_1 e_0^2 c Z_1^2}{2\pi R_o l}\frac{K_0(\kappa_o R_o)}{K_1(\kappa_o R_o)} + \frac{(N_{1T} - N_1)e_0^2 \tilde{c} Z_1^2}{2\pi R_i l}\frac{I_0(\kappa_i R_i)}{I_1(\kappa_i R_i)} = 0 \quad (21)$$

Introducing the Bjerrum length $l_B = e_0^2/(4\pi\epsilon\epsilon_0 kT)$, the Debye length inside the tube $l_D^i = 1/\kappa_i$, and the Debye length outside the tube $l_D^o = 1/\kappa_o$, we find that the electrostatic part of eq 21 can be rewritten in the form

$$kT\ln\frac{N_1(N_i - N_{1T} + N_1)}{(N_o - N_1)(N_{1T} - N_1)} + \alpha_1 - \alpha_2 - \beta_1 + \beta_2 + kT\frac{2N_1 l_B l_D^o Z_1^2}{R_o l}\frac{K_0(\kappa_o R_o)}{K_1(\kappa_o R_o)} + kT\frac{2(N_{1T} - N_1)l_B l_D^i Z_1^2}{R_i l}\frac{I_0(\kappa_i R_i)}{I_1(\kappa_i R_i)} = 0 \quad (22)$$

For the sake of simplicity we take $\xi_i^* = \xi_i$ for $i = 1,2$. The value $\xi_i \sim 20kTa$, where a is the surface area of one lipid molecule, was estimated for isotropic lipid molecules in a nearly flat bilayer membrane.[14] With increasing membrane curvature, intrinsic curvatures, and anisotropy of the lipid molecules, the value of ξ_i may be strongly increased. The values of ξ_i can be even larger for proteins and glycolipids.[35,29]

3. Results

Figure 3 shows the number of constituents of the first type (for $Z_1 = 0$) in the outer layer of the tube (N_1) as a function of the intrinsic mean curvature $H_{m,1}$. We assumed that the intrinsic mean curvature $H_{m,1}$ and the intrinsic curvature deviator $D_{m,1}$ of the membrane constituents of the first type are equal, that is, $D_{m,1} = H_{m,1}$. The value N_1 is shown for three different intrinsic curvatures $H_{m,2} = D_{m,2}$. The radius of the tube is $R = 40$ nm;

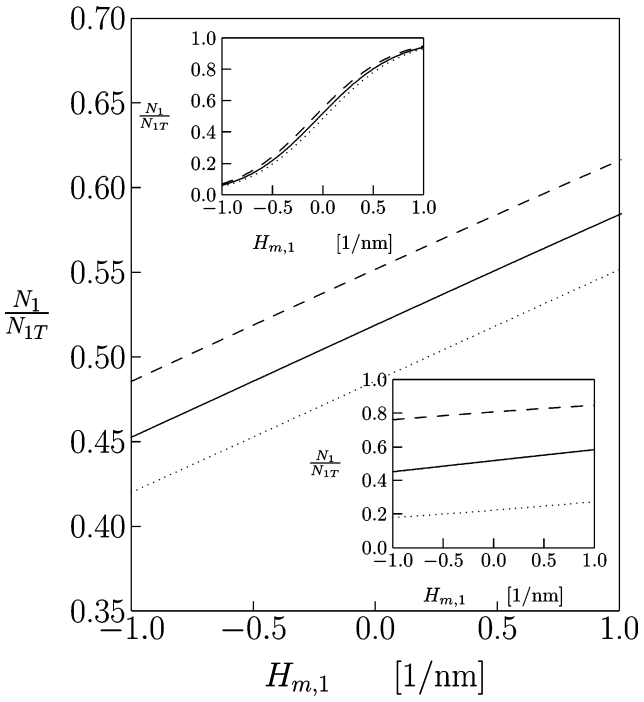

Figure 3. Number of constituents of first type in the outer layer of the tube N_1 as a function of the intrinsic mean curvature $H_{m,1}$ ($H_{m,1} = D_{m,1}$) for $Z_1 = 0$. The following intrinsic curvatures were chosen: $H_{m,2} = D_{m,2} = 0$ (normal line), $H_{m,2} = D_{m,2} = 0.5$/nm (dotted line), and $H_{m,2} = D_{m,2} = -0.5$/nm (dashed line). The model parameters are $R = 40$ nm, $N_{1T} = 100$ per 1 nm length of the tube, $\delta = 3$ nm, $a = 0.6$ nm^2, $\xi_1 = \xi_2 = 20kTa$ and the surface area of one lipid molecule $a = 0.6$ nm^2. Inset (top): N_1 as a function of $H_{m,1}$, where $\xi_1 = 200\ kTa$, $\xi_2 = 20kTa$. Inset (bottom): N_1 as a function of $H_{m,1}$, where $\xi_1 = 20kTa$, $\xi_2 = 200kTa$. We assume $\xi_i = \xi_i^*$ for $i = 1,2$.

the total number of molecules of the first type is $N_{1T} = 100$ per 1 nm length of the tube. We see that N_1 increases as a function of the intrinsic curvature $H_{m,1}$ for all three cases. For a given $H_{m,1}$, the value of N_1 decreases with increasing $H_{m,2}$. The insets of Figure 3 show N_1 as a function of the intrinsic mean curvature $H_{m,1}$ for different values of the constants ξ_1 and ξ_2. It can be seen that an increase of the interaction constant ξ_1 increases the slope of the dependence of N_1 on $H_{m,1}$. In contrast, an increase of the interaction constant ξ_2 decreases the slope of the dependence of N_1 on $H_{m,1}$.

Figure 4 shows the number of constituents of the first type in the outer layer of the tube (N_1) as a function of the intrinsic mean curvature $H_{m,1}$ for different values of the bulk concentrations of counterions inside and outside the tube and different valencies of the membrane constituents. For the sake of simplicity, we assumed $D_{m,1} = H_{m,1}$ and $H_{m,2} = D_{m,2} = 0$. The space inside and outside the tube is filled with electrolyte solutions of different ionic strengths. The constituents of the first type have valencies $Z_1 = 1$ or $Z_1 = 2$. For comparison, the case is also presented where the constituents are uncharged ($Z_1 = 0$). The total number of constituents of the first type is fixed. The radius of the tube is $R = 40$ nm. In all cases, N_1 increases with increasing intrinsic curvature $H_{m,1}$. The dependence of N_1 on $H_{m,1}$ is influenced by the electrostatic interactions; a decrease of the ionic strength outside the tube causes a decrease of N_1 in the outer layer. A decrease of the ionic strength inside the tube causes an increase of N_1 in the outer layer. These effects are pronounced for increasing valency of the membrane constituents of the first type (see Figure 4 for $Z_1 = 2$).

The counterion concentration profiles inside and outside the charged tube are shown in Figure 5. The calculated number of

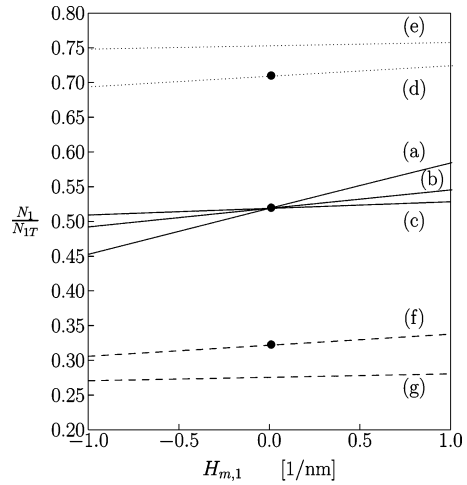

Figure 4. Number of constituents of first type in the outer layer of the tube N_1 as a function of the intrinsic mean curvature $H_{m,1}$ ($H_{m,1} = D_{m,1}$) for different values of the bulk concentrations of counterions inside the tube n_d^i and outside the tube n_d^o and different valencies of the membrane constituents of first type Z_1: $n_d^i = 0.1$ mol/l, $n_d^o = 0.1$ mol/l, $Z_1 = 1$ (b) and $Z_1 = 2$ (c); $n_d^i = 0.01$ mol/l, $n_d^o = 0.1$ mol/l, $Z_1 = 1$ (d) and $Z_1 = 2$ (e); $n_d^i = 0.1$ mol/l, $n_d^o = 0.01$ mol/l, $Z_1 = 1$ (f) and $Z_1 = 2$ (g). For comparison the case is also shown where the electrostatic effects are not taken into account (a). The model parameters are $R = 40$ nm, $N_{1T} = 100$ per 1 nm length of the tube, $H_{m,2} = D_{m,2} = 0$, $\delta = 3$ nm, $a = 0.6$ nm^2, $\xi_1 = \xi_2 = 20kTa$. We assume $\xi_i = \xi_i^*$ for $i = 1,2$.

constituents of the first type in the outer and the inner layers is also shown (Figure 5). The profiles are calculated for three different combinations of bulk values of counterion concentrations outside and inside the tube. For each combination, the number of constituents of the first type in the outer layer (N_1) was calculated (in Figure 4 these situations are indicated with points at $H_{m,1} = D_{m,1} = 0$). For each situation, from the given N_1, the surface charge densities in the inner and outer layers of the tube were calculated (eqs 17 and 15). From these surface charge densities, the concentration profiles were calculated (eqs A.12 and A.16). In the case of equal bulk values of the counterion concentrations outside and inside the tube ($n_d^o = n_d^i$), the concentrations of couterions at the inner and the outer surfaces are approximately equal. A small difference between the concentrations of couterions at the inner and those at the outer surfaces corresponds to different inner and outer area surfaces of the tube. The decreased counterion concentration in the center of the tube (Figures 4, dotted line) causes a decrease of the counterion concentration at the inner charged surface, which causes a decreased number of constituents of the first type in the inner membrane layer. While the number of constituents of the first type is fixed, the decrease in their number in the inner layer is compensated by their increase in the outer layer. In order to fulfill the electro-neutrality condition, this increase further causes an increase of the concentration of counterions near the outer surface of the tube. Analogously, the decreased bulk counterion concentration outside the tube (Figure 5, dashed line) causes a decrease of counterion concentration at the outer charged membrane surface, a decrease of the number of the constituents of the first type in the outer membrane layer, an increase of the number of constituents of the first type in the inner layer, and an increase of the counterion concentration near the inner charged membrane surface.

Figure 6 shows the number of constituents of the first type in the outer layer of the tube (N_1) as a function of the bulk concentration of counterions (and coions) in the inner (n_d^i) and the outer solution (n_d^o), respectively. It can be seen that in the

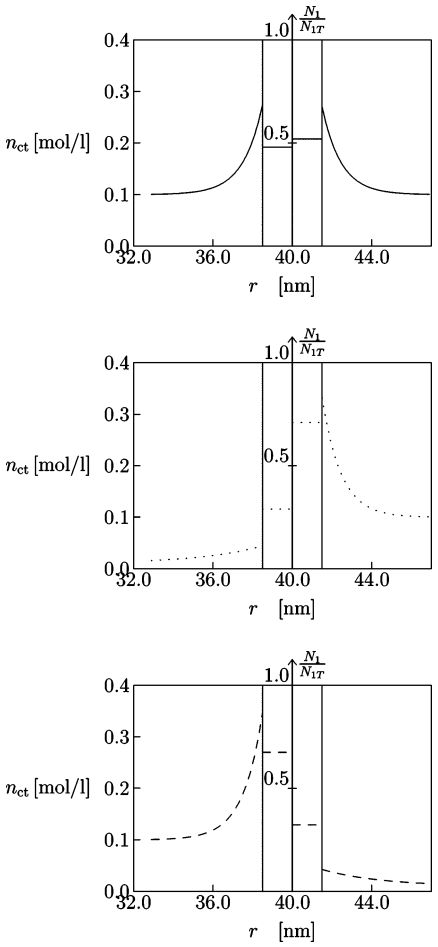

Figure 5. Concentration of counterions n_{ct} as a function of the radial coordinate r for different values of the bulk concentrations of counterions inside the tube n_d^i and outside the tube n_d^o: $n_d^i = 0.1$ mol/l, $n_d^o = 0.1$ mol/l, $\sigma^o = 0.0319$ C/m^2, $\sigma^i = 0.0318$ C/m^2 (normal lines); $n_d^i = 0.01$ mol/l, $n_d^o = 0.1$ mol/l, $\sigma^o = 0.0435$ C/m^2, $\sigma^i = 0.0193$ C/m^2 (dotted lines); and $n_d^i = 0.1$ mol/l, $n_d^o = 0.01$ mol/l, $\sigma^o = 0.0198$ C/m^2, $\sigma^i = 0.0449$ C/m^2 (dashed lines); $1C = 1As$. The surface charge densites σ^o and σ^i are obtained from eqs 15 and 17 where the numbers N_1 correspond to the points in Figure 4. The fraction of the constituents of first type in the outer and inner layers is also presented. The model parameters are $R = 40$ nm, $N_{1T} = 100$ per 1 nm length of the tube, $\epsilon = 78.5$, $T = 296$ K, and $\delta = 3$ nm.

outer layer of the tube the number N_1 decreases with increasing bulk counterion concentration n_d^i for a fixed bulk concentration $n_d^o = 0.1$ mol/l. In contrast, the number N_1 increases with increasing bulk counterion concentration n_d^o at a fixed bulk concentration $n_d^i = 0.1$ mol/l. For small ξ_i, the intrinsic curvatures of the membrane constituents do not qualitatively change the dependence of N_1 on the bulk concentration of counterions. A large ξ_1 value of constituents of the first type strongly influences the dependence of N_1 on the bulk concentration of counterions.

Figure 7 shows the electrostatic free energy as a function of the radius of the tube R for two different mean intrinsic curvatures of the molecules of the first type $H_{m,1}$. We assume $H_{m,1} = D_{m,1}$. The total number of molecules of the first type $N_{1T} = 100$ per $l_s = 1$ nm length of the tube. In order to ensure the fixed surface of the tube, the length of the segment l_s of the tube was adjusted according to the equation $R \cdot l_s = 40$ nm$\cdot$1 nm. It can be seen that the electrostatic free energy first decreases, reaches a minimum, and then increases with increasing radius of the tube. For fixed intrinsic curvatures of the

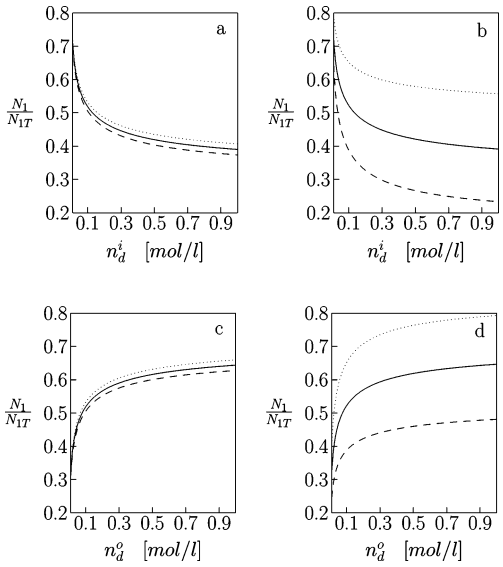

Figure 6. Number of constituents of the first type in the outer layer of the tube (N_1) as a function of the bulk counterion concentration in the outer (a,b) and in the inner solution (c,d) for different intrinsic curvatures of constituents of first type and for two different constants $\xi_1 = 20kTa$ (a,c) and $\xi_1 = 200kTa$ (b,d). The following intrinsic curvatures of constituents of first type were chosen $H_{m,1} = D_{m,1} = 0$ (normal line) $H_{m,1} = D_{m,1} = 0.5$/nm (dotted line) and $H_{m,1} = D_{m,1} = -0.5$/nm (dashed line). The total number of constituents of first type was set to $N_{1T} = 100$ per 1 nm length of the tube. The model parameters are $H_{m,1} = D_{m,1} = 0$, $R = 40$ nm, $\delta = 3$ nm, $a = 0.6$nm^2, the bulk concentration of counterions outside the tube $n_d^o = 0.1$ mol/l (a,c), and the bulk concentrations of counterions in the center $n_d^i = 0.1$ mol/l (b,d).

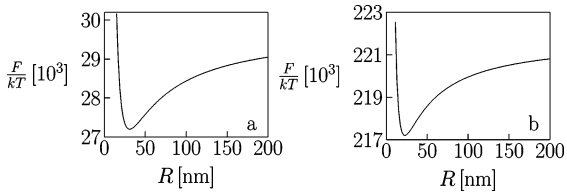

Figure 7. Electrostatic free energy as a function of the radius of the tube R. The following intrinsic curvatures of constituents of the first type were chosen: $H_{m,1} = D_{m,1} = 0.3$/nm (a) and $H_{m,1} = D_{m,1} = 0.5$/nm (b). The model parameters are the length of the tube $l = 1000$ nm, $N_{1T} = 100$ per 1 nm length of the tube, $H_{m,2} = D_{m,2} = 0.1$/nm, $n_d^i = 0.01$ mol/l, $n_d^o = 0.1$ mol/l, $Z_1 = 1$, $\delta = 3$ nm, $a = 0.6$ nm^2, $\xi_1 = \xi_2 = 20kTa$. We assume $\xi_i = \xi_i^*$ for $i = 1,2$.

molecules of the second type, the electrostatic free energy increases with increasing intrinsic mean curvature $H_{m,1}$. Figure 8 shows the energetic most favorable radius R_{eq} of the tube as a function of the intrinsic mean curvature $H_{m,1}$. We assume $H_{m,1} = D_{m,1}$. The radius R_{eq} is determined by the radius of the tube at which the absolute minimum of the electrostatic free energy is reached. The dependence R_{eq} on $H_{m,1}$ is shown for three different intrinsic curvatures $H_{m,2} = D_{m,2}$. We see that the most favorable radius R decreases with increasing intrinsic mean curvatures $H_{m,1}$ of the molecules of the first type. The decrease of R_{eq} as a function $H_{m,1}$ is pronounced for $H_{m,2} = D_{m,2} = 0.5$/nm.

4. Discussion and Conclusion

In the present work, we described the two component cylindrical bilayer which exists inside and outside a membrane in contact with an electrolyte solution composed of monovalent counterions and coions. The model takes into account (i) the

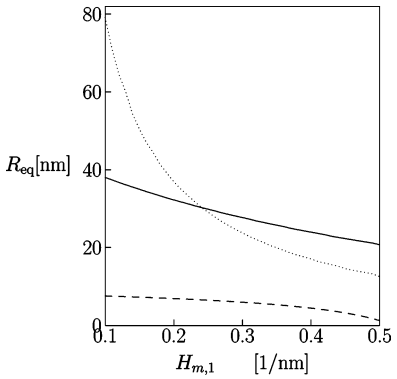

Figure 8. Energetic most favorable radius R_{eq} of the tube as a function of the intrinsic mean curvature $H_{m,1}$ ($H_{m,1} = D_{m,1}$) for $Z_1 = 1$. The following intrinsic curvatures were chosen: $H_{m,2} = D_{m,2} = 0$ (normal line), $H_{m,2} = D_{m,2} = 0.5$/nm (dotted line), and $H_{m,2} = D_{m,2} = -0.5$/nm (dashed line). The model parameters are $N_{1T} = 100$ per 1 nm length of the tube, $\delta = 3$ nm, $a = 0.6$ nm^2, $n_d^i = 0.01$ mol/l, $n_d^o = 0.1$ mol/l, $\xi_1 = \xi_2 = 20kTa$ and the surface area of one lipid molecule $a = 0.6$ nm^2.

energy of electrostatic interaction between the charged tube and the electrolyte solution, (ii) the membrane bending energy with the contribution of spontaneous curvature of its constituents and the energy due to the intrinsic (anisotropic) shape of the membrane constituents, and (iii) the free energy contribution due to the configurational entropy of the membrane constituents. The distribution of constituents of the first type between the two layers of the membrane was studied.

For the sake of simplicity, our approach assumed a fixed surface area per constituent. The anisotropy of the constituents was one of the contributions to the asymmetry of the constituents between the two layers of the membrane. Contrary to our assumption, Israelachvili et al.[28] also minimized the free energy with respect to the surface area per lipid molecule in the outer and inner layers. This was also one of the major lipid properties that determined the asymmetry.[28] A similar approach was used by Heinrich et al.[27] where counterbalanced translocation lipid fluxes between membrane layers produced changes in the number of lipids within the monolayer. This induced a lateral compression in the cytoplasmic layer and an expansion in the outer layer. This process was described by the lateral interaction energy, which is an expansion to the second-order regarding the relative area changes of a single lipid molecule.

An acknowledged and widely used description of the electrostatic interaction is given by the PB theory[41−43] in which the ions are treated as point charges in a dielectric continuum enclosed by a uniformly charged surface. For a monovalent salt, the predictions of PB theory are found to agree well with experiments and simulations.[40] In this work, we used the linearized PB theory,[33] where it is assumed that for one particle the electrostatic potential energy $e_0\Phi$ is small compared to the thermal energy kT. Let us note that the linearized PB theory is justified for potentials smaller than 25 mV at room temperature. In our calculations, the maximal obtained potential is approximately 50 mV for a surface charge density $\sigma^m = 0.038$ C/m^2, bulk concentrations $n_d^m = 0.1$ mol/l, and monovalent constituents of the membrane ($Z = 1$). These values of the potential exceed the limit of the validity of linearized PB theory. But in most of our cases, we have lower surface charge densities than σ^m, as well as lower bulk concentrations than n_d^m, leading to a potential below 50 mV where the linearized PB theory is justified. The radius of the tube $R = 40$ nm is large enough for the concentration of counterions as well as of coions along the tube axes to reach the bulk value.[44,45]

First, we discuss the results for the case where the electrostatic effects are not taken into account. Our calculations for a tube in contact with water showed that the membrane constituents of the first type for $Z_1 = 0$ with positive intrinsic mean curvature and curvature deviator $H_{m,1} = D_{m,1}$ prefer the outer layer of the tube, while the constituents of the first type with negative intrinsic mean curvature and curvature deviator $H_{m,1} = D_{m,1}$ prefer the inner layer of the tube. Constituents with no internal curvatures are uniformly distributed between two layers, where the different number of constituents between the two layers is the consequence of different area surfaces between the outer and the inner layers. In the case of constituents with no internal curvatures, approximately 52% of lipids occupy the outer layer of the tube (Figure 3). The constituents of second type with negative intrinsic mean curvatures and curvature deviator $H_{m,2} = D_{m,2}$ additionally increase the fraction of lipids with $H_{m,1} = D_{m,1}$ in the outer layer, because the shape of the constituents of the second type with negative $H_{m,2} = D_{m,2}$ favor the inner layer and the flip of constituents of the first type from the inner layer to the outer layer is forced. Analogously, constituents of the second type with positive intrinsic curvatures $H_{m,2} = D_{m,2}$ decrease N_1 in the outer layer, because they favor the outer layer of the tube and the flip of the constituents of the first type into the inner layer is forced. The situation drastically changes with increasing constants ξ_1 and ξ_2. In the limit of a very large constant ξ_1, all of the constituents of the first type with positive intrinsic curvatures $H_{m,1} = D_{m,1}$ would occupy the outer layer, while all constituents of the second type with negative intrinsic curvatures $H_{m,1} = D_{m,1}$ would occupy the inner layer. The reason is the large constant for constituents of the first type (in our case, $\xi_1 = 200kTa$) which favors the presence of constituents of the first type (top inset of Figure 3). If we increase the constant ξ_2, the majority of the constituents of the second type with positive intrinsic curvatures $H_{m,2} = D_{m,2}$ would occupy the outer layer, and they would force the constituents of the first type to occupy the inner layer; therefore, the number of these constituents in the outer layer would decrease (bottom inset of Figure 3). At large ξ_2, the majority of the constituents of the second type with negative intrinsic curvatures $H_{m,2} = D_{m,2}$ would occupy the inner layer, and they would force the constituents of the first type to occupy the outer layer (bottom inset of Figure 3). We can state that constituents like proteins, glycolipids, or small complexes of molecules (inclusions) with larger constants may have considerable influence on the asymmetry of the constituents between the leaflets of the bilayer (bottom and top insets of Figure 3).

Our prediction of an asymmetric distribution of strongly anisotropic constituents of the second type in the membrane (bottom inset of Figure 3) is in line with recent experimental results obtained on monosialoganglyoside (G_{M1})−dipalmitoylphosphatidylcholine (DPPC) mixed small unilamellar vesicles (SUV).[30] Using the inverse contrast variation method in small-angle neutron scattering, combined with small-angle X-ray scattering and dynamic light scattering, we found the predominant location of GM1 in the outer lipid layer to be due to the intrinsic shape of GM1. On the basis of its large head group,[46] sphingolipid GM1 is assumed to have positive intrinsic curvatures, that is, $C_{1,m} > 0$ and $C_{2,m} > 0$. Repulsive interactions between the negatively charged bulky head groups of GM1 and the water molecules attracted to the hydrophilic head group of GM1 additionally increase the effective size of the head groups of GM1 and therefore also their intrinsic curvatures $C_{1,m}$ and $C_{2,m}$.

Our prediction of an asymmetric distribution of strongly anisotropic constituents of the second type in the membrane is also in line with recent simulations. The simulation has been made[47] where the effect of the asymmetry in the transbilayer lipid distribution on the dynamics of phase separation in fluid vesicles was investigated. It was shown that this asymmetry set a spontaneous curvature for the domains that alter the morphology of the system.

In the following, we discuss the results of the calculations for the situation where the tube outside and inside is in contact with an electrolyte solution composed of monovalent counterions and coions. The constituents of the first type are isotropic or weakly anisotropic. For such membrane constituents, we showed that the reservoir of counterions outside and inside the tube influences the distribution of constituents of the first type in the outer and inner membrane bilayers (Figure 5). The increase of the electrolyte bulk concentration outside (inside) the tube forces constituents of the first type from the inner (outer) layer to flip into the outer (inner) layer. For very small intrinsic curvatures and small interaction constants ξ_i of constituents of the first type, the decrease of the bulk value of the counterion concentration from 0.1 mol/L in the outer solution to 0.01 mol/L in the inner solution causes 20% of the constituents to flip from the inner to the outer leaflet of the membrane. Similarly, an increase of the bulk concentration from 0.01 mol/L in the outer solution to 0.1 mol/L in the inner solution causes 20% of the constituents to flip from the outer to the inner leaflet of the membrane. The asymmetric transmembrane distribution of membrane constituents of the first type is the consequence of the difference between the ionic strength in the outer solution and that of the inner solution. This asymmetry of the constituents of the first type is pronounced for those constituents which possess more than one elementary charge; for example, for divalent (trivalent) constituents, 26% (28%) flip from the inner to the outer leaflet of the membrane if the bulk value of the counterion concentration is 0.1 mol/L in the outer solution and is 0.01 mol/L in the inner solution. An asymmetric distribution of constituents with valencies larger than 1 causes even greater asymmetry in the surface charge density between the two leaflets. We also showed that N_1 monotonously depends on the electrolyte bulk concentrations inside and outside the tube (Figure 6). The increase (descrease) of N_1 in the outer (inner) layer of the tube is the result of the increased (decreased) counterion concentration outside (inside) the tube. In order to fulfill the electro-neutrality condition, the increase of counterions in the outer solution increases the number of constituents of the first type in the outer layer of the tube.

For the constituents of the first type with large intrinsic curvatures and large interaction constants, the electrostatic interaction between the electrolyte solution and the constituents of the first type, as well as the intrinsic shape of the constituents, influence the transmembrane distribution. The constituents of the first type with negative mean curvature and curvature deviator $H_{m,1} = D_{m,1}$ can even partially reduce the transmembrane asymmetry between the two leaflets caused by the asymmetric ionic strength between the inner and the outer solutions. But the asymmetric transmembrane distribution of constituents of the first type caused by the asymmetric ionic strength between the inner and the outer solutions is pronounced for constituents with positive mean curvature and curvature deviator $H_{m,1} = D_{m,1}$.

Also, the variation of the free energy with respect to the radius of the tube R was made. The dependence of the electrostatic free energy on the radius of the tube was analyzed. The absolute minimum of the electrostatic free energy determines the energetic most favorable radius of the tube. The particles of the first type with large intrinsic curvature $H_{m,1} = D_{m,1}$ and therefore small intrinsic radius favor vesicle shapes with a small equilibrium radius. The addition of particles of the second type with large $H_{m,2} = D_{m,2}$ pronounces the decrease of radius R_{eq}. On the contrary, negative intrinsic curvatures $H_{m,2} = D_{m,2}$ weaken the decrease of R_{eq}. We showed (see Figure 7) that the tube of length 1000 nm has the energy barrier of approximately few 1000 kT for the case of inclusions with an intrinsic curvature deviator of 0.3 nm^{-1}. This energy barrier is large compared with the thermal fluctuation energy. It was estimated that the thermal fluctuation energy lies between 100 kT and 500 kT for bending rigidities between 10^{-20} J and 10^{-19} J.[48] This estimation of the fluctuation energy hints that our tubular structures are stable.

In this work, we restricted our theoretical consideration to the stable tubular structures in the regime of high lateral membrane tension in the tubes where the membrane fluctuations (and/or undulations) around the average tubular shape are largely suppressed.[38] Such large membrane tensions may be induced by a strong pulling force, as for example by inner supporting rod-like cytoskeleton filaments.[9,10] In accordance in cellular systems, most of the thin membrane protrusions are not undulated.[49,50] The stability of tubular membrane protrusions can be ensured also by accumulation of anisotropic membrane components in the membrane tubular protrusions where no pulling force is needed to stabilize the tubular membrane structure.[15,5] However, the theoretical description of the transmembrane distribution of membrane constituents in such membrane systems is beyond the scope of the present work. In accordance with our assumption of the prescribed cylindrical shape, we also assumed that the lateral distribution of each type of membrane components is homogeneous. This is presumed for each of the bilayer leaflets separately. The nonhomogeneous lateral distribution of the molecular components in each leaflet of the bilayer would lead to the undulation of the tube;[18,51,52] that is, the membrane shape and composition are mutually dependent.[52−54] In this case, the membrane components would accumulate into regions with distinct compositions and curvatures. If the membrane is composed of isotropic and anisotropic components, then the saddle-like anisotropic membrane components would accumulate in the favorable saddle-like neck regions of the undulated tube.[52]

Biological membranes have a much more complicated structure. The two monolayers of the biological membrane are comprised of various lipids. For the red blood cell membrane, it was shown that aminophosphatides (phosphatidylethanolamine and phosphatidylserine) are mainly in the cytoplasmic monolayer, while the choline derivatives (phosphatidylcholine and sphingomyelin) are mainly in the external monolayer.[55,56,49] Of the mentioned phospholipid molecules, only phosphatidylserine molecules are charged. These charged molecules are located in the inner layer of the bilayer and may contribute to the lipid asymmetry of the membrane on the basis of interaction with the cytoskeletal protein, spectrin. The binding affinity of spectrin to lipid bilayers comprised of phosphatidylcholine and phosphatidylserine has been investigated.[57] It was suggested[57] that the positively charged surface domain of the protein (although the protein possesses a net negative charge) interacts with the negatively charged lipids. But it was also shown that the affinity

of purified spectrin for phosphatidylserine containing vesicles was not significantly different from that for phosphatidylcholine vesicles.[57,58]

In summary, our model of bilayer nanotubes is based on a phenomenological free energy expression which involves the electrostatic interaction between the charged tube and the electrolyte solution, the membrane bending with the contribution of the spontaneous curvature of the constituents and the deviatoric contribution of the anisotropic membrane constituents, and the configurational entropy of the membrane constituents. The minimization of the free energy resulted in the calculated transmembrane distribution of molecules in two component bilayer nanotubes. We showed that the asymmetric transmembrane distribution of the first/second type (charge/uncharged) of membrane constituents is the result of the interplay between the intrinsic anisotropy of membrane constituents, the electrostatic interaction between the ions in the electrolyte solution, and the charged constituents of the membrane. Strongly anisotropic uncharged constituents contribute essentially to the asymmetric distribution of constituents between the two leaflets of the membrane. The asymmetric transmembrane distribution of weakly anisotropic charged constituents is driven by the electrostatic interaction between the ions in the electrolyte solution and the charged membrane constituents.

Appendix A: The Linearized PB Theory in Cylindrical Geometry

We consider a charged tube in contact with a solution of a symmetric monovalent electrolyte. The electric double layer inside the tube (concave case) and outside the tube (convex case) is considered.

For electrostatic energies small compared with the thermal energy, $|e_0\Phi| \ll kT$, where Φ is the electrostatic potential, the electric double layer can be described by the linearized PB equation[59]

$$\Delta\Psi = \kappa^2\Psi \tag{A.1}$$

where $\Psi = e_0\Phi/kT$ is the reduced electrostatic potential and $\kappa^{-1} = \sqrt{\epsilon\epsilon_0 kT/(2n_d N_A e_0^2)}$ is the Debye length, ϵ is the dielectric constant of the solution, ϵ_0 is the permittivity of a vacuum, T is the temperature, k is the Boltzmann constant, n_d is the bulk concentration of counterions (and coions), N_A is Avogadro's number, and e_0 is the elementary charge. The Laplace operator in cylindrical geometry is given by

$$\Delta = \frac{1}{r}\frac{\partial}{\partial r}\left(r\frac{\partial}{\partial r}\right) + \frac{1}{r^2}\frac{\partial^2}{\partial\varphi^2} + \frac{\partial^2}{\partial z^2} \tag{A.2}$$

where r is the radial coordinate, φ is the azimuthal angle, and z is the coordinate along the tube axis.

The solution of eq A.1 can be represented by a product $\Psi(r,\varphi,z) = R(r)\phi(\varphi)Z(z)$, where $R(r)$ depends only on r, $\phi(\varphi)$ depends only on φ, and $Z(z)$ depends only on z. For a uniformly charged and very long tube, the differential equation eq A.1 reduces to the differential equation for the radial part of the electrostatic potential

$$\frac{1}{r}\frac{d}{dr}\left(r\frac{dR(r)}{dr}\right) = \kappa^2 R(r) \tag{A.3}$$

Multiplying eq A.3 by r^2 and performing the derivation, we get

$$r^2\frac{d^2R(r)}{dr^2} + r\frac{dR(r)}{dr} - \kappa^2 r^2 R(r) = 0 \tag{A.4}$$

The solution of differential eq A.3 is[60]

$$R(r) = AI_0(\kappa r) + BK_0(\kappa r) \tag{A.5}$$

where I_0 and K_0 are the modified Bessel function and the hyperbolic Bessel function of order 0, respectively. The constants A and B are determined from the boundary conditions.

In the **concave** case, the inner surface of the charged tube is in contact with the inner electrolyte solution. The boundary conditions for the reduced potential inside the tube are

$$\left.\frac{d\Psi(r)}{dr}\right|_{r=0} = 0 \tag{A.6}$$

$$\left.\frac{d\Psi(r)}{dr}\right|_{r=R_i} = \frac{\sigma_i e_0}{\epsilon\epsilon_0 kT} \tag{A.7}$$

where σ_i is the surface charge density of the inner surface of the tube, $1/\kappa_i$ is Debye length inside the tube, and R_i is the inner radius of the tube. The boundary condition (A.7) reflects the electroneutrality of the inner surface of the charged tube and the solution inside the tube

$$\int \rho_i dV + \oint \sigma_i dS = 0 \tag{A.8}$$

where ρ_i is the volume charge density of the inner solution. The first integral in eq A.8 represents the charge of the solution while the second integral represents the charge of the inner layer of the tube. Taking into account the Poisson equation $\Delta\Phi = -\rho_i/\epsilon\epsilon_0$ and the Gauss theorem in eq A.8, we obtain the boundary condition (A.7).

The first boundary condition (eq A.6) gives $B = 0$, while from the second boundary condition (eq A.7) the constant A was calculated. Inserting the constants A and B into eq A.5, we obtain the electrostatic potential inside the tube

$$\Psi(r) = \frac{\sigma_i e_0}{kT\epsilon\epsilon_0\kappa_i}\frac{I_0(\kappa_i r)}{I_1(\kappa_i R_i)} \tag{A.9}$$

where I_1 is the modified Bessel function of order 1.

The concentration of counterions inside the tube is given by the Boltzmann distribution

$$n_{ct}^i = n_d^i e^{-\Psi(r)} \tag{A.10}$$

where n_d^i is the bulk concentration of counterions and coions inside the tube, that is, in the center of the tube. In the linearized PB theory, the exponent in eq A.10 can be expanded in the potential up to first order

$$n_{ct}^i = n_d^i(1 - \Psi(r)) \tag{A.11}$$

Inserting eq A.9 into eq A.11, we obtain

$$n_{ct}^i = n_d^i\left(1 - \sigma_i\frac{4\pi\, l_B}{e_0\kappa_i}\frac{I_0(\kappa_i r)}{I_1(\kappa_i R_i)}\right) \tag{A.12}$$

where $l_B = e_0^2/(4\pi\epsilon\epsilon_0 kT)$ is the Bjerrum length and n_d^i is the concentration of counterions and coions along the tube axis.

In the **convex** case, the outer surface of the charged tube is in contact with the outer electrolyte solution. The boundary conditions for the reduced potential outside the tube are

$$\left.\frac{d\Psi(r)}{dr}\right|_{r=R_{cell}} = 0 \tag{A.13}$$

$$\left.\frac{d\Psi(r)}{dr}\right|_{r=R_o} = -\frac{\sigma_o e_0}{\epsilon\epsilon_0 kT} \tag{A.14}$$

Here, we summarize the solution for the electrostatic potential[40]

$$\Psi(r) = \frac{\sigma_o e_0}{kT\epsilon\epsilon_0\kappa_o}\frac{K_0(\kappa_o r)}{K_1(\kappa_o R_o)} \tag{A.15}$$

and the concentration of counterions outside the charged tube

$$n_{ct}^o = n_d^o\left(1 - \sigma_o\frac{4\pi\, l_B}{e_0\kappa_o}\frac{K_0(\kappa_o r)}{K_1(\kappa_o R_o)}\right) \tag{A.16}$$

where K_1 is the modified Bessel function of order 1, $1/\kappa_o$ is Debye length outside the tube, σ^o is the surface charge density of the outer surface of the tube, R_o is the outer radius of the tube, and n_d^o is the concentration of counterions and coions at $r = R_{cell}$.

Similarly, as in the concave case, the boundary condition (A.14) in the convex case reflects the electroneutrality of the outer surface of the charged tube and the solution outside the tube

$$\int \rho_o\, dV + \oint \sigma_o\, dS = 0 \tag{A.17}$$

where ρ_o is the volume charge density of the inner solution. The first integral in eq A.17 represents the charge of the solution outside the tube, while the second integral represents the charge of the outer layer of the tube. Here we already take into account the electroneutrality of the inner surface of the charged tube and the solution inside the tube.

References and Notes

(1) Karlsson, A.; Karlsson, R.; Karlsson, M.; Cans, A. S.; Strömberg, A.; Ryttsen, F.; Orwar, O. *Nature* **2001**, *409*, 150.

(2) Iglič, A.; Hägerstrand, H.; Bobrowska-Hägerstrand, M.; Arrigler, V.; Kralj-Iglič, V. *Phys. Lett. A* **2003**, *310*, 493.

(3) Sun, M.; Graham, J. S.; Hegedüs, B.; Marga, F.; Zhang, Y.; Forgacs, G. *Biophys. J.* **2005**, *89*, 4320.

(4) Rustom, A.; Saffrich, R.; Markovic, I.; Walther, P.; Gerdes, H. H. *Science* **2004**, *303*, 1007.

(5) Gimsa, U.; Iglič, A.; Fiedler, S.; Zwanzig, M.; Kralj-Iglič, V.; Jonas, L.; Gimsa, J. *Mol. Membr. Biol.* **2007**, *24*, 243.

(6) Iglič, A.; Lokar, M.; Babnik, B.; Slivnik, T.; Veranič, P.; Hägerstrad, H.; Kralj-Iglič, V. *Blood Cell. Mol. Dis.* **2007**, *39*, 14.

(7) Miyata, H.; Nishiyama, S.; Akashi, K.; Kinosita, K. *Proc. Natl. Acad. Sci. U.S.A.* **1999**, *96*, 2048.

(8) Boulbitch, A. A. *Phys. Rev. E: Stat. Phys., Plasmas, Fluids, Relat. Interdiscip. Top.* **1998**, *57*, 2123.

(9) Emsellem, V.; Cardoso, O.; Tabeling, P. *Phys. Rev. E: Stat. Phys., Plasmas, Fluids, Relat. Interdiscip. Top.* **1998**, *58*, 4807.

(10) Derenyi, I.; Jülicher, F.; Prost, J. *Phys. Rev. Lett.* **2002**, *88*, 238101.

(11) Dabora, S. L.; Sheetz, M. P. *Cell* **1988**, *54*, 27.

(12) Evans, E.; Bowman, H.; Leung, A.; Needham, D.; Tirell, D. *Science* **1996**, *273*, 933.

(13) Raucher, D.; Sheetz, M. P. *Biophys. J.* **1999**, *77*, 1992.

(14) Kralj-Iglic, V.; Iglic, A.; Gomiscek, G.; Arrigler, V.; Hägerstrand, H. *J. Phys. A: Math. Gen.* **2002**, *35*, 1533.

(15) Kralj-Iglic, V.; Hägerstrand, H.; Veranic, P.; Jezernik, K.; Babnik, B.; Gauger, D. R.; Iglic, A. *Eur. Biophys. J.* **2005**, *34*, 1066.

(16) Iglič, A.; Hägerstrand, H.; Veranic, P.; Plemenitas, A.; Kralj-Iglic, V. *J. Theor. Biol.* **2006**, *240*, 368.

(17) Miao, L.; Fourcade, B.; Rao, M.; Wortis, M.; Zia, R. K. P. *Phys. Rev. E: Stat. Phys., Plasmas, Fluids, Relat. Interdiscip. Top.* **1991**, *43*, 6843.

(18) Tsafrir, I.; Caspi, Y.; Guedeau, M. A.; Arzi, T.; Stavans, J. *Phys. Rev. Lett.* **2003**, *91*, 138102.

(19) Elsner, M.; Hashimoto, H.; Nilsson, T. *Mol. Membr. Biol.* **2003**, *20* (3), 221.

(20) Sprong, H.; van der Sluijs, P.; van Meer, G. *Nat. Cell. Biol.* **2001**, *2*, 504.

(21) Davis, D. M. *Sci. Am.* **2006**, *294* (2), 48.

(22) Huttner, W. B.; Zimmerberg, J. *Curr. Opin. Cell. Biol.* **2001**, *13*, 478.

(23) Bergelson, L. D.; Barsukov, L. I. *Science* **1977**, *197*, 224.

(24) Williamson, P.; Antia, R.; Schlegel, R. A. *FEBS Lett.* **1987**, *219*, 316.

(25) Calvez, J. Y.; Zachowski, A.; Herrmann, A.; Morrot, G.; Devaux, P. F. *Biochemistry* **1988**, *27*, 5666.

(26) Brumen, M.; Heinrich, R.; Müller, P. *Eur. Biophys. J.* **1993**, *22*, 213.

(27) Heinrich, R.; Brumen, M.; Jaeger, A.; Mueller, P.; Herrmann, A. *J. Theor. Biol.* **1997**, *185*, 295.

(28) Israelachvili, J. N.; Mitchell, D. J.; Ninham, B. W. *Biochim. Biophys. Acta* **1977**, *470*, 185.

(29) Iglič, A. A.; Kralj-Iglic, V. *FEBS Lett.* **2004**, *9*, 574/1−3.

(30) Hirai, M.; Iwase, H.; Hayakawa, T.; Koizumi, M.; Takahashi, H. *Biophys. J.* **2003**, *85*, 1600.

(31) McLaughlin, S. *Annu. Rev. Biophys. Chem.* **1989**, *18*, 113.

(32) Cevc, G. *Biochim. Biophys. Acta* **1990**, *1031−3*, 311.

(33) Verwey, E. J.; Overbeek, J. Th. G. *Theory of Stability of Lyophobic Colloids*; Elsevier Publishing Company: New York, 1948.

(34) Fournier, J. B. *Phys. Rev. Lett.* **1996**, *76*, 4436.

(35) Kralj-Iglic, V.; Svetina, S.; Zeks, B. *Eur. Biophys. J.* **1996**, *24*, 311.

(36) Kralj-Iglic, V.; Heinrich, V.; Svetina, S.; Zeks, B. *Eur. Phys. J. B* **1999**, *10*, 5.

(37) Kralj-Iglic, V.; Babnik, B.; Gauger, D. R.; May, S.; Iglic, A. *J. Stat. Phys.* **2006**, *125*, 727.

(38) Fournier, J. B.; Galatola, P. *Phys. Rev. Lett.* **2007**, *98*, 018103.

(39) Israelachvili, J. N. *Intermolecular and surface forces*; Academic Press: London, 1997.

(40) Evans, D. F.; Wennerström, H. *The Colloidal Domain: Where Physics, Chemistry, Biology, and Technology Meet*; VCH Publishers: New York, 1994.

(41) Gouy, M. G. *J. Phys. Radium (Paris)* **1910**, *9*, 457.

(42) Chapman, D. L. *Philos. Mag.* **1913**, *6*, 475.

(43) Oosawa, F. *Polyelectrolytes*; Marcel Dekker: New York, 1970.

(44) Bohinc, K.; Gimsa, J.; Kralj-Iglic, V.; Slivnik, T.; Iglic, A. *Bioelectrochemistry* **2005**, *67*, 91.

(45) Bohinc, K.; Iglic, A.; Slivnik, T. *Electrotech. Rev.* **2005**, *72* (2−3), 107.

(46) Hirai, M.; Iwase, H.; Arai, S.; Takizawa, T.; Hayashi, K. *Biophys. J.* **1998**, *74*, 1380.

(47) Laradji, M.; Kumar, P. B. S. *Phys. Rev. E.: Stat. Phys., Plasmas, Fluids, Relat. Interdiscip. Top.* **2006**, *73*, 040901.

(48) Seifert, U. *Adv. Phys.* **1997**, *46*, 13.

(49) Alberts, B.; Johnson, A.; Lewis, J.; Raff, M.; Roberts, K.; Walter, P. *Molecular Biology of the Cell;* Garland Science: New York, 2002.

(50) Bray, D. *Cell Movements*; Garland Publishing: New York, 2000.

(51) Shemesh, T.; Luini, A.; Malhotra, V.; Burger, K. N. J.; Kozlov, M. M. *Biophys. J.* **2003**, *85*, 3813.

(52) Iglic, A.; Babnik, B.; Bohinc, K.; Fosnaric, M.; Hägerstrand, H.; Kralj-Iglic, V. *J. Biomech.* **2007**, *40*, 579.

(53) Markin, V. S. *Biophys. J.* **1981**, *36*, 1.

(54) Gozdz, W. T.; Gompper, G. *Phys. Rev. Lett.* **1998**, *80*, 4213.

(55) Rothman, J. E.; Tsai, D. K.; Dawidowicz, E. A.; Lenard, *J. Biochem.* **1976**, *15*, 2361.

(56) Rothman, J. E.; Lenard, J. *Science* **1977**, *195*, 743.

(57) O'Toole, P. J.; Morrison, I. E.; Cherry, R. J. *Biochim. Biophys. Acta* **2000**, *1466*, 39.

(58) Sikorski, A. F.; Hanus-Lorenz, B.; Jezierski, A.; Dluzewski, A. R. *Acta Biochim. Polon.* **2000**, *47*, 565.

(59) Andelman, D. In *Handbook of Biological Physics*, Vol. 1; Lipowsky, R., Sackmann, E.; 1995; p 603.

(60) Jackson, J. D. *Classical Electrodynamics*; John Wiley: New York, 1998.